

# Electrochemical oxidation-reduction and determination of urea at enzyme free PPY-GO electrode

Harish Mudila<sup>1,2</sup>, Parteek Prasher<sup>3</sup>, Sweta Rana<sup>2</sup>, Beena Khati<sup>4</sup>, and M.G.H. Zaidi<sup>2,\*</sup>

<sup>1</sup>Department of Chemistry, G. B. Pant University of Agriculture & Technology, Pantnagar, Uttarakhand-263145, India

<sup>2</sup>Department of Chemistry, Lovely Professional University, Phagwara, Punjab-144411, India

<sup>3</sup>Department of Chemistry, University of Petroleum and Energy Studies, Dehradun, Uttarakhand-248007, India-

<sup>4</sup>Department of Biotechnology, DBS Campus Bhimtal Kumaun University, Nainital, Uttarakhand-263136, India

## Article Info

Received 16 April 2017

Accepted 7 July 2017

## \*Corresponding Author

E-mail: mghzaidi@gmail.com

Tel: +919458177485

## Open Access

DOI: <http://dx.doi.org/10.5714/CL.2018.26.088>

This is an Open Access article distributed under the terms of the Creative Commons Attribution Non-Commercial License (<http://creativecommons.org/licenses/by-nc/3.0/>) which permits unrestricted non-commercial use, distribution, and reproduction in any medium, provided the original work is properly cited.

## Abstract

This manuscript explains the effective determination of urea by redox cyclic voltammetric analysis, for which a modified polypyrrole-graphene oxide (PPY-GO, GO 20% w/w of PPY) nanocomposite electrode was developed. Cyclic voltammetry measurements revealed an effective electron transfer in 0.1 M KOH electrolytic solution in the potential window range of 0 to 0.6 V. This PPY-GO modified electrode exhibited a moderate electrocatalytic effect towards urea oxidation, thereby allowing its determination in an electrolytic solution. The linear dependence of the current vs. urea concentration was reached using square-wave voltammetry in the concentration range of urea between 0.5 to 3.0  $\mu\text{M}$  with a relatively low limit of detection of 0.27  $\mu\text{M}$ . The scanning electron microscopy was used to characterize the morphologies and properties of the nanocomposite layer, along with Fourier transform infrared spectroscopy. The results indicated that the nanocomposite film modified electrode exhibited a synergistic effect, including high conductivity, a fast electron-transfer rate, and an inherent catalytic ability.

**Key words:** Polypyrrole, graphene oxide, polysulphone, urea, cyclic voltammetry, electrocatalytic effect, limit of detection.

## 1. Introduction

The rapid increase in farming and industrial activities had led to the increased presence of urea in water. Urea  $[(\text{NH}_2)_2\text{CO}]$  is one of the chief human nitrogen-based metabolic wastes. The concentration of urea in blood lies between 2.5–7 mM for healthy individuals. The urea concentration in serum or urine indicates kidney diseases and diabetes, and its analysis in clinical laboratories is very frequent [1,2]. In addition, the monitoring of urea is essential for a number of applications, including food processing, agricultural processes, and environmental protection. However, the urea quantification uses conventional methods, such as spectrophotometric, potentiometry, and piezoelectricity [2,3], which are expensive and time consuming. Therefore, it is very important to develop simple, sensitive, and accurate methods for detecting urea. A variety of analytical methods have been developed and used to analyze urea in aqueous samples. As a result, voltammetric sensors have become an excellent alternative for detecting various analytes, including urea. Since urea is electroactive and most of the electroanalytical techniques are selective, highly sensitive, time-saving, inexpensive, have a wide dynamic range, and a quick response, electrochemical techniques have been used to determine urea as a strong alternative to the other methods. Various forms of modified electrodes have been used for electrochemical studies of urea because of their unusual characteristics [1,2, 4-10]. These modified electrodes showed good sensitivity, selectivity, stability, and excellent detection, even at a low concentration, because of the unique electronic



<http://carbonlett.org>

pISSN: 1976-4251

eISSN: 2233-4998

Copyright © Korean Carbon Society

and catalytic properties of the electroactive materials used.

Inherently conducting polymers are useful in modern research due to their highly conductive properties when doped and their concurrent mechanical flexibility [4,11,12]. PPY has been used as a sensor/biosensor by itself or with other analysts for the effective sensing of protein [13], DNA [14], certain drugs [15-17], hydrogen peroxide [18], uric acid [19], ascorbic acid [20-22], nitrite [23], and glucose [24]. Similarly, GO and its composites have been applied as sensors for paracetamol [25], 4-nitrophenol [26],  $Hg^{2+}$  [27], hemoglobin [28], and escherichia coli [29]. Most of the applied urea sensors rely on urease along with sensing material due to which these sensors are highly sensitive and selective. In contrast, the use of enzymes in the matrix makes the method complicated, time consuming, and expensive. The activity and sensitivity of such enzyme based sensors are knocked back with changes in the chemical and thermal environments, humidity, and toxicity. Various electrochemical enzyme free sensing studies have been used for the successful detection of various analytes while overcoming the drawbacks of enzyme associated sensors [3,30-32]. However, certain drawbacks such as multistep synthesis, reduced sensitivity, and non-environmental benign states associated with these enzyme free sensors still prevail. In this respect, to minimize such drawbacks, a modified PPY-GO based sensor was prepared. As a conducting material PPY-GO is considered to have excellent electronic transport properties and high electrocatalytic activities, and it has been investigated as a potential electrode material for electrochemical supercapacitors [33]. In general, the large surface area, excellent conductivity, and strong mechanical strength of GO and the polymerized chain of PPY have motivated others to apply an enzyme free PPY-GO nanocomposite as a urea sensor.

The aim of the present work is to improve urea determination by using conducting material. This manuscript describes a PPY-GO electrochemical sensor that was fabricated with polypyrrole and graphene oxide (GO 20% w/w of PPY) on stainless steel electrodes (SS), while the electrochemical properties of the sensor were investigated by cyclic voltammetry (CV) and square wave voltammetry (SWV). This sensor can be used for the ultrasensitive determination of urea in wastewater or body waste. This matrix has cyclic stability, hence resulting in sensors that have enhanced sensitivity and versatility. The results show that a PPY-GO modified electrode exhibits excellent performance for detecting urea and shows a limit of detection (LOD) of 0.27  $\mu M$ . In contrast, the previous works of Piccinini *et al.* and Prissanaroon *et al.* suggested a higher value of LOD for GO and PPY for urea [34,35].

## 2. Materials and Method

### 2.1. Starting materials

Commercially available pyrrole (>99%), polysulfone (Mw; 16X103), CTAB, (>99%), chlorosulfonic acid (>99%), and graphite were purchased from Sigma Aldrich. Other chemicals and solvents were obtained from Fine Chemicals India.

### 2.2 Preparation of GO and SPS

GO was prepared based on a modified Hummers method [33]. The as-prepared GO had similar properties compared to reduced GO, which had saturable absorption and a long range C=C backbone [36]. The SPS was used as a binder and one of the ingredients in the matrix used for sensing was synthesized through sulfonating polysulfone (PS) with chlorosulfonic acid [39].

### 2.3. In-situ preparation of PPY-GO nanocomposite

The process of synthesizing the electroactive nanocomposite was performed in a thermostatically controlled glass reactor assembly comprised of a three necked flask equipped with a mechanical stirrer, thermometer, and dropping funnel charged with a solution of  $FeCl_3$  (30 mL,  $1.85 \times 10^{-2}$  mol/dL). A suspension of pyrrole (0.28M, 30 mL) in de-ionized water was stabilized with a surfactant (CTAB, 1.145 g) while the requisite concentration of GO was placed in the flask. The polymerization was initiated through adding a  $FeCl_3$  solution at a rate of 1mL/ min to the contents while under a constant mechanical stirring at a rate of 600 rpm over 24 h at  $10 \pm 1^\circ C$  [40]. The prepared nanocomposite was isolated in a yield (%) ranging at 95 through centrifugation at 6000 rpm over 10 min, followed by filtration and repeated washing with de-ionized water until the unreacted  $FeCl_3$  and surfactants were completely removed to obtain a jet black material (Fig. 1). This material was dried at  $50 \pm 1^\circ C/400$  mmHg over 8 h in a vacuum oven.

### 2.4. Modification of working electrodes

The stainless steel (316-SS) was used as a substrate on which the electroactive material binded with SPS was applied, degreased with acetone, and subjected to surface oxidation at  $50 \pm 1^\circ C$  for over 1 h. A composition of PPY-GO (20% w/w, 65 mg) along with graphite (10 mg) and SPS (5 g/dL) in N-Methyl-2-pyrrolidone (NMP) was sonicated for over 15 min.

The sonicated material (50 mL) was applied over a SS substrate in the working area of  $1 cm^2$  and the contents were allowed to stand at room temperature for 2 h, followed by vacuum drying at  $100^\circ C/400$  mm Hg for 48 h. This has resulted in working electrodes with a mass thickness of electroactive materials by  $5 \pm 1$  mg over the 316-SS substrate (Fig. 2).

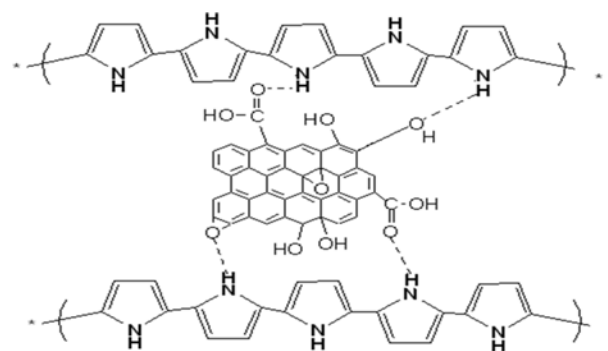


Fig. 1. PPY-GO Composite

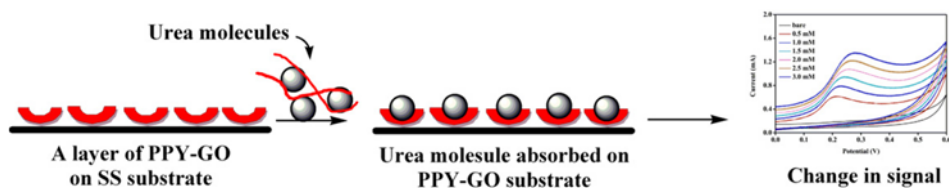


Fig. 2. Probable working of PPY-GO electrode

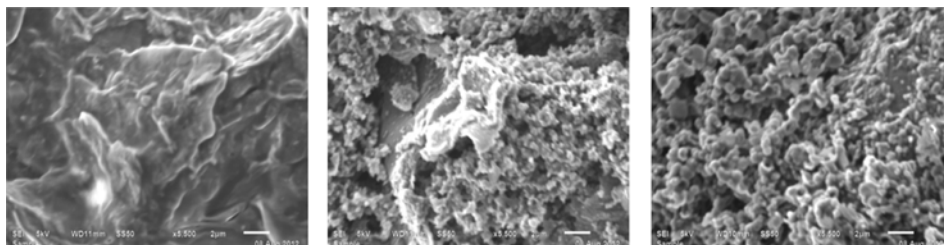


Fig. 3. SEM micrographs of PPY, GO, and PPY-GO, respectively

## 3. Results and Discussion

### 3.1. Surface and structural characterization

SEM micrographs at 5.0 KX, 2 mm were used to provide qualitative and surface features information about the exfoliation of GO onto the matrix of PPY. Fig. 3 illustrates comparatively the images of GO, PPY particles, and PPY-GO composite material. The SEM of GO reveals a characteristic fluffy flaky appearance and rough surface characteristics with non-uniform grains [37]. PPY has shown a clear phase separation with specific porous morphology associated with a spheroid grain-like structure. The synthesized PPY-GO micrographs clearly represent a phase separation with flaky morphology clearly indicating the intercalation of GO into PPY layers.

### 3.2. Spectroscopic analysis

Fig. 4 shows the comparative FT-IR spectra of GO, PPY, and PPY-GO. The synthesized GO indicates characteristic  $\nu$  O-H absorption at  $\sim 3333$   $\text{cm}^{-1}$ , as well as  $\nu$  COOH,  $1613$   $\text{cm}^{-1}$  (remaining  $\text{sp}^2$  character),  $1378$   $\text{cm}^{-1}$  ( $\nu$  COC),  $1221.20$   $\text{cm}^{-1}$  (C-O for epoxide), and  $1033$   $\text{cm}^{-1}$  ( $\nu$  COH), respectively. The PPY shows characteristic absorptions corresponding to  $1500$   $\text{cm}^{-1}$  ( $\nu$  C=C) and  $1475$   $\text{cm}^{-1}$  ( $\nu$  C-N) for symmetric ring stretching. The broadband at  $1300$   $\text{cm}^{-1}$  corresponds to an in-plane deformation of C-H and C-N. The peaks near  $1190$   $\text{cm}^{-1}$  and  $922$   $\text{cm}^{-1}$  represent the doping state of PPY with  $\text{Fe}^{3+}$ , and the peak at  $1050$   $\text{cm}^{-1}$  is attributed to the N-H deformation the band at  $901$   $\text{cm}^{-1}$  shows C-H out of plane deformation vibration. The band at  $\sim 3450$   $\text{cm}^{-1}$  is attributed to the ( $\nu$  N-H). FT-IR spectrum of the PPY-GO derived from PPY and GO (20% w/w) [33, 40]. When compared to the IR spectra of the individual GO sheet and PPY, all of the peaks also appeared in the composite, which implies that the PPY chains integrated with GO to form the composite. It is well observed that in the composite some bands of PPY shifted to a lower wavenumber due to the constrained growth polymerization in the presence of GO.

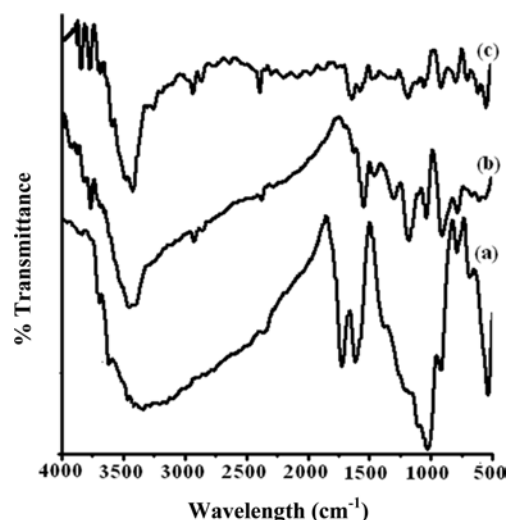


Fig. 4. FT-IR of GO (a) PPY (b) PPY-GO nanocomposite (c)

### 3.3. XRD analysis

The diffraction peaks observed at  $2\theta$  were used to calculate the spacing by using Bragg's equation:

$$d = \frac{n\lambda}{2\sin\theta} \quad (1)$$

where  $\lambda = 0.154$  nm and  $n=1$ , the XRD of GO reduces in the  $2\theta = 11.83^\circ$  ( $d = 3.37$  Å for graphite) with a gallery spacing of  $7.47$  Å [33, 38]. Due to its amorphous nature, no crystalline peak was observed in the case of PPY, which showed  $2\theta = 27.26^\circ$  and a gallery spacing ( $d$ ) of  $3.63$  Å.

A steep decrease in  $2\theta$  was observed along with an increase in the gallery spacing, which can be attributed to the GO intercalation to PPY with  $2\theta = 26.43$  to  $23.63^\circ$  while the gallery spacing ( $d$ ) was found to be in the range of  $3.37$  to  $3.76$  Å. This rendered characteristic diffused XRD spectra indicating an

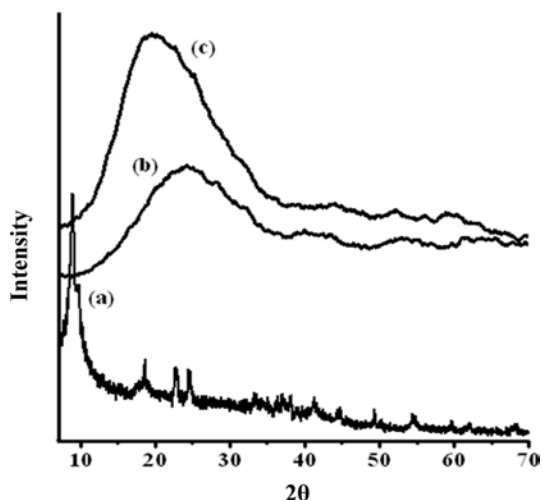


Fig. 5. XRD pattern of (a) GO, (b) PPY, (c) PPY-GO nanocomposite

amorphous character that has some crystallinity as the percentage of the crystalline material in the material (Fig. 5).

### 3.4. Voltammetric measurement

The  $C_s$  was found to be ranging from 1073.64 F/g for PNCs synthesized at a GO concentration of 20% w/w at a sweep rate ranging from 0.001 V/s, which was much higher than that of GO and pure PPY 342.794 F/g and 89.832 F/g, respectively (Fig. 6c; As also introduced in our previous [33], Fig. 6). The specific capacitance ( $C_s$ ) of the active materials was calculated from the voltammetric charges by the CV curve, by means of relation:

$$C_s(F/g) = \frac{qa + |qc|}{2m\Delta V} \quad (2)$$

where “qa” and “qc” are the voltammetric charges on anodic and cathodic scans in the capacitive potential region ( $\Delta V$ ) and “m” is the mass of active material. The sensing of analyte, i.e., urea, was done with cyclic voltammetry and the square wave voltammetry technique. Electrochemical measurements were carried out on IVIUM potentiostat-galvanostat Netherlands BV

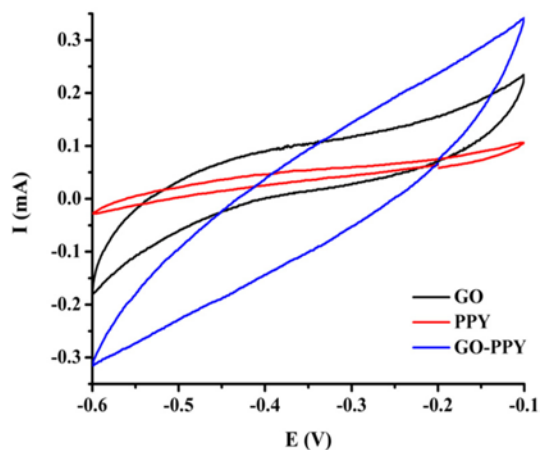


Fig. 6. CV curves for various electroactive materials

at a current compliance of 10 mA, ranges of voltage compliance from 0.0 to 0.6 V, and at a scan rate (V/s) of 0.01 by using a three electrode cell assembly with reference to the Ag/AgCl electrode. Pt foil with a 1 cm<sup>2</sup> area was used as a counter electrode and commercially available 316-SS electrode as a working electrode in 1M KOH electrolytic solution was maintained at a pH=5.8 via a 0.1M potassium phosphate buffer (KPB). Mudila *et al.* [41] found KOH to be a superior electrolyte for electrochemical studies when compared to Na<sub>2</sub>SO<sub>4</sub>. The stability of the electrode material was found to be good even after numerous cycles [33]. This study justifies the use of modified electrodes for several runs without removing them from an electrolytic sample. This study thus authenticates the economic importance of these electrodes when compared to other such sensors.

### 3.5. Cyclic Voltammetry (CV)

The full cyclic voltamogram of urea was recorded in the potential range of -1.3 to 0.6 V (Fig. 7). The anodic part of the voltammogram was characterized by the occurrence of the anodic peaks corresponding to the electro-oxidation of the urea while the cathodic part of the cyclic voltammograms was characterized by the occurrence of cathodic peaks corresponding to the electro-reduction of the urea. Along with the redox peaks of the analyte, the substrate also showed corresponding redox peaks in the potential window range.

This indicates that the redox peaks in the curve can be attributed to the direct electron transfer behaviors of urea molecules immobilized in the PPY-GO nanocomposite film. In the presence of PPY-GO, the coated electrode produced much larger background currents and visible redox peaks. This difference was attributed to the high surface area and good electrical conductivity of PPY-GO, which are believed to enhance electron transfer. The electrochemical redox process is purely diffusion controlled on the surface of PPY-GO, i.e., there are impulsive movements in the electroactive species from higher to lower concentration regions. The cathodic peak current ( $I_{p,c}$ ) and the anodic peak current ( $I_{p,a}$ ) were located at about -0.785 mA and 0.183 mA, which correspond to -0.124 V and 0.404 V cathodic and anodic potential, respectively, at a scan rate of 0.01 V/s and a 0.5  $\mu$ M concentration (Fig. 7).

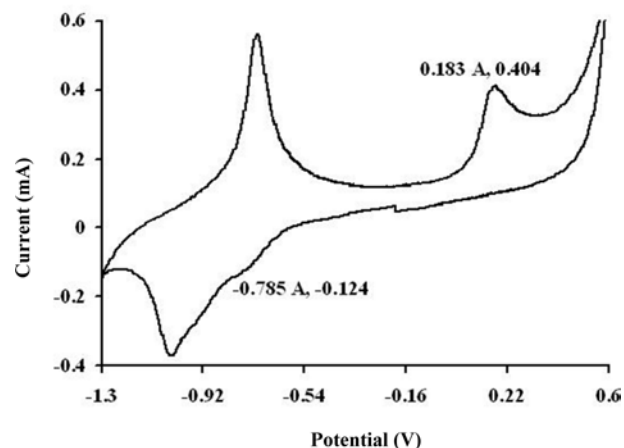


Fig. 7. Anodic and Cathodic peaks corresponding to analyte

### 3.6. Effect of concentration of analyst

For the electrolytic solution, 0.5  $\mu\text{M/L}$  of the urea solution was injected for every cyclic scan for six successive turns. Each subsequent injection of analyte depicted an enhanced peak in the scan (Fig. 8), which indicated the sensing of analyte by the PPY-GO nanocomposite. At an applied potential of -0.1 V and with an increased concentration of urea, the response current increased immediately and a fast response time was estimated. This can be attributed to the fast diffusion of urea within the PPY-GO nanocomposite and excellent electron transfer behavior of GO within the PPY film on the SS electrode surface.

Fig. 9 shows the relation of the variation diagram of response current at the successive additions of the urea samples. The response was linear in range from 0.5 to 3  $\mu\text{M}$ . To assess reproducibility, six sequential measurements of 0.5  $\mu\text{M}$  were performed.

### 3.7. Influence of scan rate

Fig. 10 shows the effect of the square root of the scan rate on the CV response of the urea in a supporting electrolyte. Both the oxidation peak current and reduction peak current showed a well linear relationship with the scan rate in the potential range

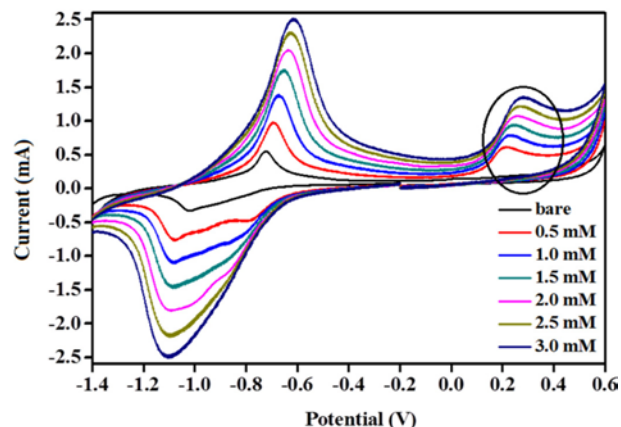


**Fig. 8.** Cyclic voltammograms of PPY-GO composite electrode in 0.1 M KOH supporting electrolyte and in the presence of different urea concentrations, at a potential scan rate 0.01 V/s and potential range of 0.0 to 0.06 V.

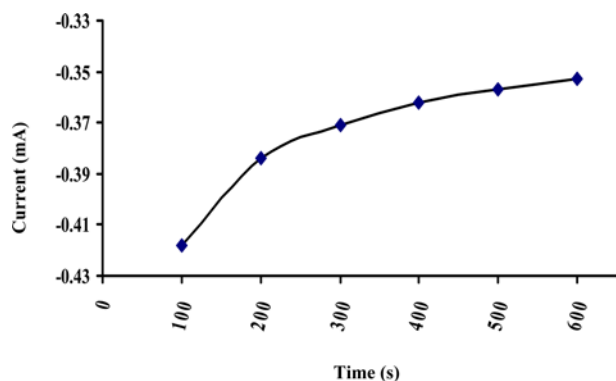


**Fig. 9.** Amperometric response at a constant potential of 0.01 V with the injecting of 0.1 mM/L urea every 100 seconds at a scan rate of 0.1 V/s.

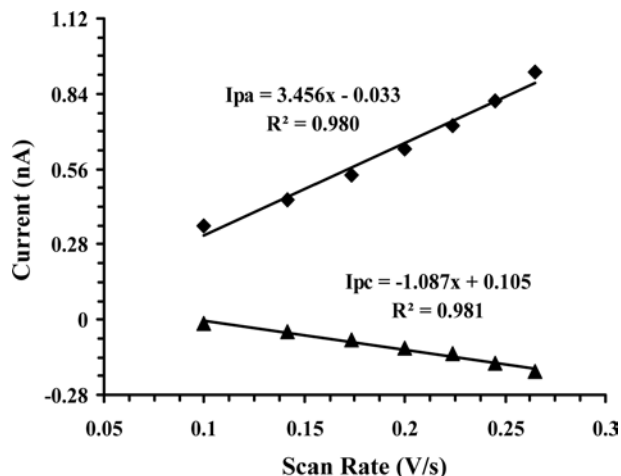


**Fig. 10.** Linear plot current vs. square root of scan rate

of 0.01 to 0.07 V. The redox peak current and peak potential increased with an increase in scan rates between 0.01–0.1 V/s, which confirmed the surface confined redox process.

### 3.8. Square-wave voltammetry (SWV)

Similar results were also obtained by using square-wave voltammetry and the voltammograms in relation with the urea concentrations presented in Fig. 11. The scan parameters were square-wave mode, a step of 5 mV, an amplitude of 100 mV, and a frequency of 2 Hz. As can be seen, the SWV peak current increased linearly with the urea concentration in the potential range of -0.4 to 0.4 V. Under optimal experimental conditions, the peak current at approximately -0.11 V varied linearly with a urea concentration in the range of 0.5–3.0  $\mu\text{M}$ . A variation in the urea concentration was found to have influenced the peak potential: the peak potential shifted towards more negative values when the concentration increased.

The limit of detection (LOD) was calculated by the following relation [42]:

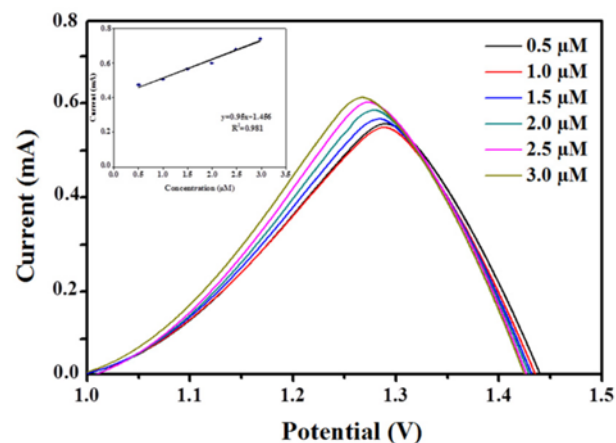


**Fig. 11.** SWV of successive additions of urea concentration. Inset: The corresponding calibration plot of SWV

$$\text{LOD} = 3 \text{ SD/S} \quad (3)$$

where “SD” is the standard deviation of the peak current (three runs) of the concentration of the linearity range (3.12  $\mu\text{M}$ ) and “S” is the slope of the related calibration equation. The LOD was calculated as 0.27  $\mu\text{M}$ . This result indicates that the modified electrode is more sensitive towards analytes in the absence of enzymes.

#### 4. Conclusion

The CV-SWV procedure for the PPY-GO electrodes provides a convenient and efficient method for the assay of urea. It was inferred that the voltammetric response in alkaline media is suitable for analytical applications. It is possible to apply the proposed electrode material for determining the amount urea in water and human waste, as it shows a low limit of detection (LOD=0.27 $\mu\text{M}$ ). Apart from this, the proposed voltammetric method for urea determination can also be useful in many different applications such as urea containing pesticides, fruit juices, solutions used in leaching experiments, and bleaching. The obtained modified electrodes are stable and highly permeable for ions, but at the same time, they fulfill the conditions needed for fast electron transfer. Due to the easy and inexpensive maintenance of renewable PPY-GO electrodes in the field, this method can be a key step in detecting urea and other analytes in environmentally important matrices by field-based voltammetry.

#### Acknowledgements

This work was supported by the DRDO under Grant No. ERIP/ER/0703649/M/01/1092 and DST Inspire Fellowship under Grant No. IF-110513.

#### References

- [1] Branzoi V, Musina A, Branzoi F. Amperometric Urea Biosensor Based Platinum Electrode Modified With A Composite Film. *Rev. Roum. Chim.*, 56(9), 883 (2011). DOI: <http://dx.doi.org/10.5772/52440>
- [2] Singh M, Verma N, Garg AK, Redhu N. Urea biosensors. *Sensors and Actuators B: Chemical, Sensors and Actuators B.* 134, 345 (2008). DOI: 10.1016/j.snb.2008.04.025
- [3] Arain M, Nafady A, Sirajuddin, Ibupoto ZH, Sherazi T, Shaikh T, Abdul Niaz AN, Willander M, Simpler and highly sensitive enzyme free sensing of urea via NiO nanostructures modified electrode. *RSC Adv.*, 6, 39001 (2016). DOI: 10.1039/C6RA00521G.
- [4] Hamilton A. The Formation and Characterisation of a Polypyrrole Based Sensor for the Detection of Urea. National University of Ireland, Maynooth, PhD Thesis (2012).
- [5] Nicolau E, Fonseca JJ, Cabrera CR. Development of a Urea Bioprobe Based on Platinized Boron-Doped Diamond Electrodes. *Electroanalysis*, 24(11), 2102 (2012). DOI: 10.1002/elan.201200459.
- [6] Manea F, Pop A, Radovan C, Malchev P, Bebeselea A, Burtica G, Picken S, Schoonman J. Voltammetric Detection of Urea on an Ag-Modified Zeolite-Expanded Graphite-Epoxy Composite Electrode. *Sensors*, 8, 5806 (2008). DOI:10.3390/s8095806
- [7] Ivanova S, Ivanov Y, Godjevargova T. Urea Amperometric Biosensors Based on Nanostructured Polypyrrole and Poly Ortho-Phenylenediamine. *Open Journal of Applied Biosensor.* 2, 12 (2013). DOI:10.4236/ojab.2013.21002.
- [8] Mondal S, Sangaranarayanan MV. A novel non-enzymatic sensor for urea using a polypyrrole-coated platinum electrode. *Sensors & Actuators: B. Chemical.* 177, 478 (2013). DOI: 10.1016/j.snb.2012.11.031
- [9] Park SH, Jin JH, Min NK, Hong SI. Poly(3-methylthiophene)-Based Urea Sensors with Planar Pt Electrodes on Silicon Substrates. *Journal of the Korean Physical Society*, 40(1),17 (2002). DOI: 10.3938/jkps.40.17
- [10] Yang JK, Ha KS, Baek HS, Lee SS, Seo ML. Amperometric Determination of Urea Using Enzyme-Modified Carbon Paste Electrode. *Bull. Korean Chem. Soc.*, 25(10), 1499 (2004). DOI: 10.5012/bkcs.2004.25.10.1499
- [11] Yoon H. Current Trends in Sensors Based on Conducting Polymer Nanomaterials. *Nanomaterials.* 3, 524 (2013). DOI: 10.3390/nano3030524
- [12] Ramanavicius A, Ramanaviciene A, Malinauskas A. Electrochemical sensors based on conducting polymer—polypyrrole. *Electrochimica Acta.*, 51(27), 6025 (2006). DOI: <http://dx.doi.org/10.1016/j.electacta.2005.11.052>
- [13] Rick J, Chou TC. Amperometric protein sensor—fabricated as a polypyrrole, poly-aminophenylboronic acid bilayer. *Biosensors and Bioelectronics*, 22, 329 (2006). DOI: 10.1016/j.bios.2006.04.007
- [14] Chen Y, Elling, Lee YL, Chong SC. A Fast, Sensitive and Label Free Electrochemical DNA Sensor. *Journal of Physics: Conference Series*, 34, 204 (2006). DOI:10.1088/1742-6596/34/1/034
- [15] Tiwari DC, Jain R, Sharma S. Electrochemically deposited polyaniline/polypyrrole polymer film modified electrodes for determination of furazolidone drug. *Journal of Scientific and Industrial Research*, 66, 1011 (2007). DOI: <http://nopr.niscair.res.in/handle/123456789/1347>
- [16] Xing X, Liu S, Yu J, Lian W, Huang J. Electrochemical sensor based on molecularly imprinted film at polypyrrole-sulfonated graphene/hyaluronic acid-multiwalled carbon nanotubes modified electrode for determination of tryptamine. *Biosens Bioelectron.* 31(1), 277 (2012). DOI: 10.1016/j.bios.2011.10.032.
- [17] Sasso L, Heiskanen A, Diazzi F, Dimaki M, Castillo-León J, Vergani M, Landini E, Raiteri R, Ferrari G, Carminati M, Sampietro M, Svendsen WE, Emneus J. Doped overoxidized polypyrrole microelectrodes as sensors for the detection of dopamine released from cell populations. *Analyst*, 138, 3651 (2013). DOI: 10.1039/c3an00085k.
- [18] Zhang T, Yuan R, Chai Y, Li W, Ling S. A Novel Nonenzymatic Hydrogen Peroxide Sensor Based on a Polypyrrole Nanowire-Copper Nanocomposite Modified Gold Electrode. *Sensors*, 8, 5141 (2008). DOI: 10.3390/s8085141
- [19] Yang G, Tan L, Shi Y, Wang S, Lu X, Bai H, Yang Y. Direct Determination of Uric Acid in Human Serum Samples Using Polypyrrole Nanoelectrode Ensembles. *Bull. Korean Chem. Soc.*, 30(2), 454 (2009). DOI: <https://doi.org/10.5012/bkcs.2009.30.2.454>
- [20] Zhuang Z, Li J, Xu R, Xiao D. Electrochemical Detection of Dopamine in the Presence of Ascorbic Acid Using Overoxidized Polypyrrole/Graphene Modified Electrodes. *Int. J. Electrochem. Sci.*, 6,

- 2149 (2011). DOI: 10.1016/j.talanta.2012.05.013
- [21] Shi W, Liu C, Song Y, Lin N, Zhou S, Cai X. An ascorbic acid amperometric sensor using over-oxidized polypyrrole and palladium nanoparticles composites. *Biosens. Bioelectron.* 38(1), 100 (2012). DOI:10.1016/j.bios.2012.05.004
- [22] Samseya J, Srinivasan R, Chang YT, Tsao CW, Vasantha VS. Fabrication and characterisation of high performance polypyrrole modified microarray sensor for ascorbic acid determination. *Anal. Chim. Acta.* 793, 11 (2013). DOI: 10.1016/j.aca.2013.06.049.
- [23] Ye D, Luo L, Ding Y, Chena Q, Liu X. A novel nitrite sensor based on graphene/polypyrrole/chitosan nanocomposite modified glassy carbon electrode. *Analyst*, 136, 4563 (2011). DOI: 10.1039/C1AN15486A
- [24] Raicopol M., Pruna A, Damian C, Pilan L. Functionalized single-walled carbon nanotubes/polypyrrole composites for amperometric glucose biosensors. *Nanoscale Research Letters*, 8, 316 (2013). DOI: 10.1186/1556-276X-8-316
- [25] Devadas B, Rajkumar M, Chen SM, Saraswathi R. Electrochemically Reduced Graphene Oxide/ Neodymium Hexacyanoferrate Modified Electrodes for the Electrochemical Detection of Paracetamol. *Int. J. Electrochem. Sci.* 7, 3339 (2012). [www.electrochemsci.org/papers/vol7/7043339.pdf](http://www.electrochemsci.org/papers/vol7/7043339.pdf)
- [26] Giribabu K, Suresh R, Manigandan R, Vijayalakshmi L, Stephen A, Narayanan V. Synthesis of reduced graphene oxide and its electrochemical sensing of 4-nitrophenol. *AIP Conference Proceedings*, 1512, 400 (2013). DOI: <http://dx.doi.org/10.1063/1.4791080>
- [27] Zhou N., J. Li, H. Chen, C. Liao and L. Chen. A functional graphene oxide-ionic liquid composites-gold nanoparticle sensing platform for ultrasensitive electrochemical detection of Hg<sup>2+</sup>. *Analyst*, 138, 1091 (2013). DOI: 10.1039/c2an36405k.
- [28] Dang X, Zheng J, Hu C, Wang S, Hu S. Hemoglobin biosensor based on reduced graphite oxide modified gold electrode array printed on paper. *Chemical Sensors*, 3(17), 1 (2013). DOI: <http://www.cognizure.com/abstract.aspx?p=107637252>
- [29] Jiang X, Chen K, Wang J, Shao K, Fu T, Shao F, Lu D, Liang J, Foda MF, Han H. Solid-state voltammetry-based electrochemical immune sensor for Escherichia coli using graphene oxide-Ag nanoparticle composites as labels. *Analyst*, 138, 3388 (2013). DOI: 10.1039/c3an00056g.
- [30] Lee JH, El-Said WA, Oh BK, Choi JW. Enzyme-free glucose sensor based on Au nanobouquet fabricated indium tin oxide electrode. *J Nanosci Nanotechnol.* 14(11), 8432 (2014). DOI:10.1166/jnn.2014.9921
- [31] Baloach QU, Tahira A, Mallah AB, Abro MI, Uddin S, Willander M, Ibupoto ZH. A Robust, Enzyme-Free Glucose Sensor Based on Lysine-Assisted CuO Nanostructures. *Sensors (Basel)*. 16(11), 1878 (2016). DOI: 10.3390/s16111878
- [32] Bai Y, Yang W, Sun Y, Sun C. Enzyme-free glucose sensor based on a three-dimensional gold film electrode. *Sensors and Actuators B: Chemical*, 134(2), 471 (2008). DOI: 10.1016/j.snb.2008.05.028
- [33] Mudila H, Zaidi MGH, Rana S, Joshi V, Alam S. Enhanced Electrocapacitive Performance of Graphene Oxide Polypyrrole Nanocomposites. *Int. J. of Chemical and Analytical Science.* 4, 139 (2013). DOI:10.1016/j.ijcas.2013.09.001
- [34] Piccinini E, Bliem C, Rozman CR, Battaglini F, Azzaroni O. Enzyme-polyelectrolyte multilayer assemblies on reduced graphene oxide field-effect transistors for biosensing applications. *Biosensors and Bioelectronics* 92, 661 (2017). DOI: <https://doi.org/10.1016/j.bios.2016.10.035>
- [35] Prissanaroon OW, Sirivat A, Pigram, PJ, Brack N. Potentiometric Urea Biosensor Based on a Urease-Immobilized Polypyrrole. *Macromolecular Symposia* 354(1), 334, (2015). DOI: 10.1002/masy.201400087.
- [36] Sobon G, Sotor J, Jagiello J, Kozinski R, Zdrojek M, Holdynski M, Paletko P, Boguslawski J, Lipinska L, Abramski KM. Graphene oxide vs. reduced graphene oxide as saturable absorbers for Er-doped passively mode-locked fiber laser. *Opt Express*. 20(17), 19463 (2012). DOI: 10.1364/OE.20.019463.
- [37] Bose S, Kim NH, Kuila T, Lau T and Lee JH. Electrochemical performance of a graphene-polypyrrole nanocomposite as a supercapacitor electrode. *Nanotechnology*, 22, 295202, 2011.
- [38] Graphene oxide and reduced graphene oxide studied by the XRD, TEM and electron spectroscopy methods. L. Stobinski, B. Lesiak, A. Malolepszy, M. Mazurkiewicz, B. Mierzwa, J. Zemek, P. Jiricek, I. Bieloshapka. *Journal of Electron Spectroscopy and Related Phenomena*. 195, 145 (2014). DOI: <http://dx.doi.org/10.1016/j.elspec.2014.07.003>
- [39] Unnikrishnan L, Madamana P, Mohanty S, Nayak SK. Polysulfone/C30B Nanocomposite Membranes for Fuel Cell Applications: Effect of Various Sulfonating Agents. *Polymer-Plastics Technology and Engineering*, 51, 568 (2012) DOI:10.1080/03602559.2012.654580
- [40] Mudila H, Rana S, Zaidi MGH, Alam S. Enhanced electrocapacitive performance and high power density of polypyrrole/graphene oxide nanocomposites prepared at reduced temperature. *Carbon Letters* 15(3), 171 (2014). DOI: <http://dx.doi.org/10.5714/CL.2014.15.3.171>
- [41] Mudila H, Joshi V, Rana S, Zaidi MGH, Alam S. Comparative electrochemical study of sulfonated polysulphone binded graphene oxide supercapacitor in two electrolytes. *Carbon Letters*, 18, 43 (2016). DOI: <http://dx.doi.org/10.5714/CL.2016.18.043>
- [42] Manea F, Pop A, Radovan C, Malchev P, Bebeselea A, Burtica G, Picken S and Schoonman J. Voltammetric Detection of Urea on an Ag-Modified Zeolite-Expanded Graphite-Epoxy Composite Electrode. *Sensors* 8, 5806, 2008. DOI: 10.3390/s8095806.